Inhibition of Angiogenesis by HC·HA, a Complex of Hyaluronan and the Heavy Chain of Inter-α-Inhibitor, Purified from Human Amniotic Membrane

Elizabeth Shay,[1] *Hua He,*[1] *Shunsuke Sakurai,*[1] *and Scheffer C. G. Tseng*[1,2]

Purpose. To determine whether antiangiogenic action of the amniotic membrane (AM) can be mediated by HC·HA, a covalent complex of hyaluronan (HA) and the heavy chain (HC) of inter-α-inhibitor, purified from AM soluble extract.

Methods. HC·HA action on viability, proliferation, attachment, death, migration, and differentiation of human umbilical vein endothelial cells (HUVECs) and neovascularization in chicken chorioallantoic membrane (CAM) was examined by MTT assay, BrdU labeling, cell proliferation assay, cell death detection ELISA, transwell assay, tube formation assay, and CAM assay.

Results. HC·HA suppressed HUVEC viability more significantly than HA and AM stromal extract, and such suppression was not mediated by CD44. HC·HA also caused HUVECs to become small and rounded, with a decrease in spreading and filamentous actin. Without promoting cell detachment or death, HC·HA dose dependently inhibited proliferation (IC_{50}, 2.3 μg/mL) and was 100-fold more potent than HA. Migration triggered by VEGF and tube formation was also significantly inhibited by HC·HA. Purified HC·HA did not contain PEDF and TSP-1 but did contain IGFBP-1 and platelet factor 4 while significantly suppressing neovascularization in CAM.

Conclusions. The antiangiogenic activity of HC·HA might explain why AM is developmentally avascular and how AM might exert an antiangiogenic action when transplanted to the ocular surface, and it might indicate a potential therapeutic effect of HC·HA in diseases manifesting pathogenic angiogenesis. Roles of IGFBP-1 and platelet factor 4 in HC·HA antiangiogenic action warrant further investigation. (*Invest Ophthalmol Vis Sci.* 2011;52:2669–2678) DOI:10.1167/iovs.10-5888

Amniotic membrane (AM), the innermost layer of the placental membrane, is composed of a simple epithelium, a basement membrane, and an avascular stroma; the mechanism for stromal avascularity remains unknown. Cryopreserved AM, in which both amniotic epithelial cells and stromal mesenchymal cells are devitalized,[1] was first advocated by Kim and Tseng[2] to help restore the corneal surface in a rabbit model of chemical injuries. Besides the reduction of inflammation and scarring, AM-transplanted corneal surfaces show reduced vascularization.[2] This antiangiogenic action has also been exploited during corneal surface reconstruction in conjunction with transplantation of corneal epithelial stem cells from the limbus.[3–5] Although transplantation of the cryopreserved AM has become a standard surgical procedure for reconstructing corneal and conjunctival surfaces damaged by a number of diseases (see Refs. 6–10 for reviews), the active component and the mechanism responsible for this antiangiogenic action remain to be elucidated.

Previously, a soluble AM extract prepared by boiling and homogenization was shown to prevent angiogenesis in a rat model of corneal neovascularization induced by alkali burn and by suppressing the viability and tube formation of the cultured human umbilical vein endothelial cells (HUVECs).[11] Recently, we biochemically purified HC·HA, a covalent complex formed by high molecular weight hyaluronan (HA) and the heavy chain (HC) of inter-α-inhibitor (IαI), from water-soluble AM extract.[12] The formation of HC·HA is mediated by the tumor necrosis factor-α–stimulated gene-6 protein (TSG-6), which catalyzes the transfer of HC from IαI to HA.[13–15] Our previous study showed that HC·HA, either purified from AM or reconstituted in vitro by mixing such defined components as HA, IαI, and TSG-6, is more potent than HA in inhibiting the viability of cultured murine macrophages and suppressing the TGF-β1 promoter activity of cultured human corneal fibroblasts.[12] The above two in vitro assays have been shown to correlate well with the anti-inflammatory[16,17] and anti-scarring[18,19] actions exerted by AM and AM extract, respectively. It remains unknown whether HC·HA purified from the AM might also exert the antiangiogenic action that has been clinically observed by AM and AM extract.

At the present time, the only known function of HC·HA is to ensure female fertility. HC·HA is the principal component of the cumulus matrix that surrounds and protects oocytes from environmental injury during and after ovulation, and it facilitates sperm attachment, penetration, and fertilization.[13,20] HA can be degraded into smaller fragments under certain physiological or pathologic conditions. Many studies have consistently shown that these fragments stimulate vascular endothelial cell proliferation, migration, collagen synthesis, sprout formation, and angiogenesis in the rat skin, myocardial infarction, and cryo-injured skin grafts by promoting the gene expression of proinflammatory and proangiogenic mediators, whereas HA inhibits inflammation and angiogenesis.[21–24] In addition to recently reported anti-inflammatory and anti-scarring actions,[12] we herein provide strong evidence that HC·HA exerts a more potent antiangiogenic action than does HA by inhibiting viability, proliferation, migration, and differentiation without promoting the detachment or death of cultured HUVECs.

From [1]TissueTech, Inc., Miami, Florida; and [2]Ocular Surface Center, Miami, Florida.

Supported by National Eye Institute/National Institutes of Health Grants R43 EY021045 and R44 EY017497, a research grant from Tissue Tech, Inc., and an unrestricted grant from Ocular Surface Research and Education Foundation, Miami, Florida.

Submitted for publication May 14, 2010; revised August 9 and October 29, 2010; accepted November 21, 2010.

Disclosure: **E. Shay**, Tissue Tech, Inc. (F, E); **H. He**, Tissue Tech, Inc. (F, E); **S. Sakurai**, Tissue Tech, Inc. (F, E); **S.C.G. Tseng**, Tissue Tech, Inc. (F, I), P

Corresponding author: Scheffer C. G. Tseng, Ocular Surface Center, 7000 SW 97 Avenue, Suite 213, Miami, FL 33173; e-mail: stseng@ocularsurface.com.

Copyright 2011 The Association for Research in Vision and Ophthalmology, Inc.

METHODS

Reagents, Antibodies, and Assays

Fibronectin (Fn), vitronectin (Vn), VEGF, a mouse monoclonal antibody (MAB1177) against human pigment epithelial-derived factor (PEDF), and human angiogenesis arrays (catalog no. ARY007) were obtained from R&D Systems (Minneapolis, MN). Type I collagen (C), extracellular matrix (Matrigel), a CD44 neutralizing antibody (clone IM7), and a normal rat IgG2b antibody were purchased from BD Biosciences (Franklin Lakes, NJ). A mouse monoclonal antibody against thrombospondin-1 (TSP-1) was purchased from EMD (San Diego, CA). A mixture of 10 μg/mL Fn and 35 μg/mL C (FNC Coating Mix) was from Athena Enzyme Systems (Baltimore, MD). Bovine serum albumin (BSA), Hoechst 33342, Triton X-100, Tween-20, and glutaraldehyde were purchased from Sigma (St. Louis, MO). A protein assay kit was from Pierce (BCA; Rockford, IL). Medical grade HA (Healon) was obtained from Abbott Medical Optics (Abbott Park, IL). A test kit for HA (Quantitative Test Kit) was obtained from Corgenix (Westminster, CO). MTT (3-[4, 5-dimethylthiazol-2-yl]-2,5-diphenyl tetrazolium bromide) assay, cell proliferation BrdU ELISA, and a cell death detection kit (Cell Death Detection ELISA^{PLUS}) were from Roche (Mannheim, Germany). Basic fibroblast growth factor (bFGF), cell proliferation assay (CyQuant), and AlexaFluor 488–conjugated phalloidin were from Invitrogen (Carlsbad, CA). Mouse anti–BrdU antibody and goat anti–mouse IgG-FITC were from Millipore (Billerica, MA). Sterilized nylon mesh (Nitex) was from Sefar (Depew, NY). Fertilized White Leghorn chicken eggs were from Charles River (Wilmington, MA).

Preparation of AM, Stromal Extract, and HC·HA

Both AM stromal extract (ASE) and HC·HA were prepared aseptically from frozen human AM obtained from Bio-Tissue, Inc. (Miami, FL), as previously described.[12] In short, after washing off the original storage medium, intact AM or AM stroma obtained by scraping with a spatula was frozen in liquid nitrogen and ground to fine particles (BioPulverizer; Biospec Products, Inc., Bartlesville, OK) followed by homogenization on ice. ASE was prepared by collecting the supernatant from the AM stromal homogenate centrifuged at 14,000*g* for 30 minutes at 4°C. For HC·HA, the supernatant collected from the AM homogenate, centrifuged at 48,000*g* at 4°C for 30 minutes, was collected and subjected to two runs of ultracentrifugation in CsCl/4 M guanidine HCl at the initial density of 1.35 g/mL (first run) and 1.40 g/mL (second run). As reported,[12] fractions designated as HC·HA contained HA (measured with the HA Quantitative Test Kit) but no detectable proteins (BCA assay). Thus, we expressed HC·HA concentration based on the HA concentration measured in the HC·HA complex. To date, we have consistently purified an average of 1.52 ± 0.26 mg HC·HA (based on HA content) per placenta from three different donors.

Culture on Different Substrates

HUVECs were maintained in the endothelial cell growth medium (ECGM) (cells and medium were from Promocell, Heidelberg, Germany) containing 1 ng/mL human basic fibroblast growth factor, 0.004 mL/mL endothelial cell growth supplement/heparin, 0.1 ng/mL epidermal growth factor, 1.0 μg/mL hydrocortisone, and 0.02 mL/mL FBS. Cells were split at 1:2 once they reached 70% to 90% confluence; cells of passages 3 to 8 were used for experiments. At room temperature, each 96-well plate was coated with FNC (64 μL/well) for 1 minute, 20 μg/mL Fn or 5 μg/mL Vn in Dulbecco's PBS for 2 hours, or 50 μg/mL C solution in 0.02 N acetic acid for 1 hour. For Fn- and Vn-coated plates, wells were blocked with 2 mg/mL heat-inactivated BSA in Dulbecco's PBS for 1 hour at 37°C. These plates were immediately seeded with cells for testing.

Attachment, Viability, Proliferation, and Death Assays

HUVECs were seeded at 4000 cells per uncoated or coated 96-well plate (high seeding density) and were cultured in ECGM with the simultaneous or sequential (after 24 hours) addition of ASE, HA, or HC·HA in PBS. For attachment, cells were cultured for 30 minutes and then washed three times with medium; the remaining attached cells were quantified with a cell proliferation assay (CyQuant). For viability, cells were cultured up to 48 hours before the MTT assay. To test the CD44 blocking effect, 50 μg/mL of a CD44 neutralizing antibody (IM7) or a rat IgG2b isotype control antibody was added 1 hour before HUVECs were seeded at 3000 cells/96-well plate or 24 hours after HUVECs were seeded at 2000 cells/96-well plate (low seeding density) with or without 25 μg/mL HC·HA or HA. For proliferation, 10 μM BrdU in ECGM was added for the last 6 hours of the culturing period before the cell proliferation ELISA BrdU assay. For death, conditioned media and cell lysates of each culture were subjected to the cell death detection (ELISA^{PLUS}; Roche) as previously described.[16,17] Each of the above tests was performed in triplicate. Data are reported as mean ± SD and analyzed with Student's *t*-test in data analysis software (Excel; Microsoft, Redmond, WA). Dose-response curves and IC_{50} values were determined with software using 4 Parameter Logistic Regression (MasterPlex; Miraibio, Alameda, CA).

Chemotaxis Assay

The inhibitory effect of HC·HA on VEGF-induced chemotaxis was tested by seeding 4×10^5 cells in the upper well of each transwell (Corning, Lowell, MA) containing ECGM with 25 μg/mL HA or HC·HA, while 10 ng/mL VEGF was added as a chemoattractant in the bottom well containing ECGM. After culturing for 4 hours, cells remaining in the upper chamber were removed by a cotton-tipped applicator. Inserts were removed, washed with PBS, and stained with crystal violet for 10 minutes. Five random 100× fields were photographed for each well, and migrated cells were counted, averaged, and compared.

Tube Formation Assay

The effect of HC·HA on the differentiation of HUVECs was determined by the tube formation assay, as previously described.[25] Briefly, 250 μL extracellular matrix (Matrigel, 9.6 mg/mL; BD Biosciences) was added to each well of a 24-well plate and allowed to polymerize at 37°C for 30 minutes. HUVECs at 50,000 cells/well were seeded onto the extracellular matrix with 25 μg/mL HA or HC·HA in ECGM supplemented with 10% FBS. After culturing for 16 hours, five random 100× fields were photographed under a phase-contrast microscope for each well, and tubes were counted, averaged, and compared with ImageJ software (developed by Wayne Rasband, National Institutes of Health, Bethesda, MD; available at http://rsb.info.nih.gov/ij/index.html).

Immunofluorescence Staining

HUVECs were seeded at 1×10^4 cells/uncoated 8-chamber slide and cultured for 48 hours. For BrdU staining, cells were fixed with Carnoy's fixative (3:1 for methanol/glacial acetic acid) for 20 minutes, permeabilized with 2 M HCl, and blocked with 0.05% Tween-20 and 2% BSA for 30 minutes before the addition of anti–BrdU antibody for 1 hour and an anti–mouse-IgG-FITC antibody for 1 hour at 37°C. For phalloidin staining, cells were fixed in 4% paraformaldehyde for 10 minutes and permeabilized with 0.2% Triton X-100 for 5 minutes. After blocking with 2% BSA for 1 hour, AlexaFluor 488–conjugated phalloidin was added for 20 minutes. The nucleus was counterstained with Hoechst 33342 dye. Images were taken with a confocal microscope (LSM 700; Zeiss, Oberkochen, Germany).

Western Blot Analysis

AM extract, pooled fractions after the first ultracentrifugation (F1) and the second (F2) ultracentrifugation, and HC·HA (each containing 2 μg HA) were electrophoresed on 4% to 15% (wt/vol) gradient acrylamide (Ready; Bio-Rad, Hercules, CA) gels under denaturing and reducing conditions. Proteins were transferred to the nitrocellulose membrane. The membrane was then blocked with 5% (wt/vol) fat-free milk in TBST (50 mM Tris-HCl, pH 7.5, 150 mM NaCl, 0.05% [vol/vol] Tween-

20) followed by sequential incubation with specific primary antibodies against PEDF or TSP-1 and their respective secondary antibodies. Immunoreactive proteins were detected with reagent (Western Lighting Chemiluminescence; PerkinElmer, Waltham, MA).

Measurement of Human Angiogenic and Antiangiogenic Factors by Protein Arrays

Angiogenic and antiangiogenic factors in human AM extract and purified HC·HA were determined by human angiogenesis arrays (each array contains 56 different candidate proteins) according to the protocol recommended by the manufacturer. Briefly, human AM extract and purified HC·HA were first centrifuged at 15,000*g* for 10 minutes at 4°C to remove particles. Then these samples were diluted with cytokine array (Array Buffer 4; R&D Systems) to make the same final concentration of HA at 25 μg/mL as used in other experiments, each with a total volume of 1.5 mL. Samples were incubated separately with the detection antibodies for 1 hour at 25°C, followed by incubation with the individual blocked membrane overnight at 4°C. After wash, the membrane was incubated with the secondary antibody, and signals were detected with chemiluminescent light exposed to x-ray film. The array data on developed x-ray film were quantitated by scanning the film on a transmission-mode scanner, and the array image file was analyzed by ImageJ software.

Antiangiogenic Activity in Vivo by HC·HA Complex Using Chicken CAM Assay

Fertilized White Leghorn chicken eggs were incubated at 37.5°C with 60% humidity. On day 3, a 1-cm diameter hole was opened in the shell. To make collagen onplants (2.07 mg/mL collagen I), the collagen I (3 mg/mL) was first neutralized before the addition of 16.7 μg/mL bFGF and 5 μg/mL VEGF with or without 1 μg/onplant high molecular weight HA or 1 μg/onplant HC·HA. For each onplant, 30 μL collagen mixture was deposited onto two layers of sterilized nylon mesh (Nitex 100/32 [Sefar]; bottom layer, 4 × 4 mm; top layer, 2 × 2 mm). The onplants were allowed to polymerize for 90 minutes at 37°C before application to the CAM of a day 8 chick embryo and were continuously incubated for 4 days, during which time the angiogenic response was monitored through a dissecting microscope (Nikon, Tokyo, Japan). At the end of the treatment period, each CAM was fixed with 0.5 mL of 25% glutaraldehyde and subjected to vessel quantitation by counting the total vessels radiating into each collagen onplant.

Statistical Analysis

Unless otherwise indicated, data are represented as the mean ± SD of three or four independent experiments, with a sample size of four or more for each condition. Student's *t*-test was performed to test statistical significance from controls. $P < 0.05$ was considered statistically significant.

Results

HC·HA Suppressed HUVEC Viability More Than ASE and HA Independently of CD44

To determine whether HC·HA purified from soluble AM extract might exert an antiangiogenic action, we seeded trypsinized HUVECs immediately with ASE (200 μg/mL protein, 2.5 μg/mL HA), 5 μg/mL HA, or 5 μg/mL HC·HA and cultured them for 48 hours. The MTT assay showed that both ASE and HC·HA significantly inhibited HUVEC viability compared with the PBS

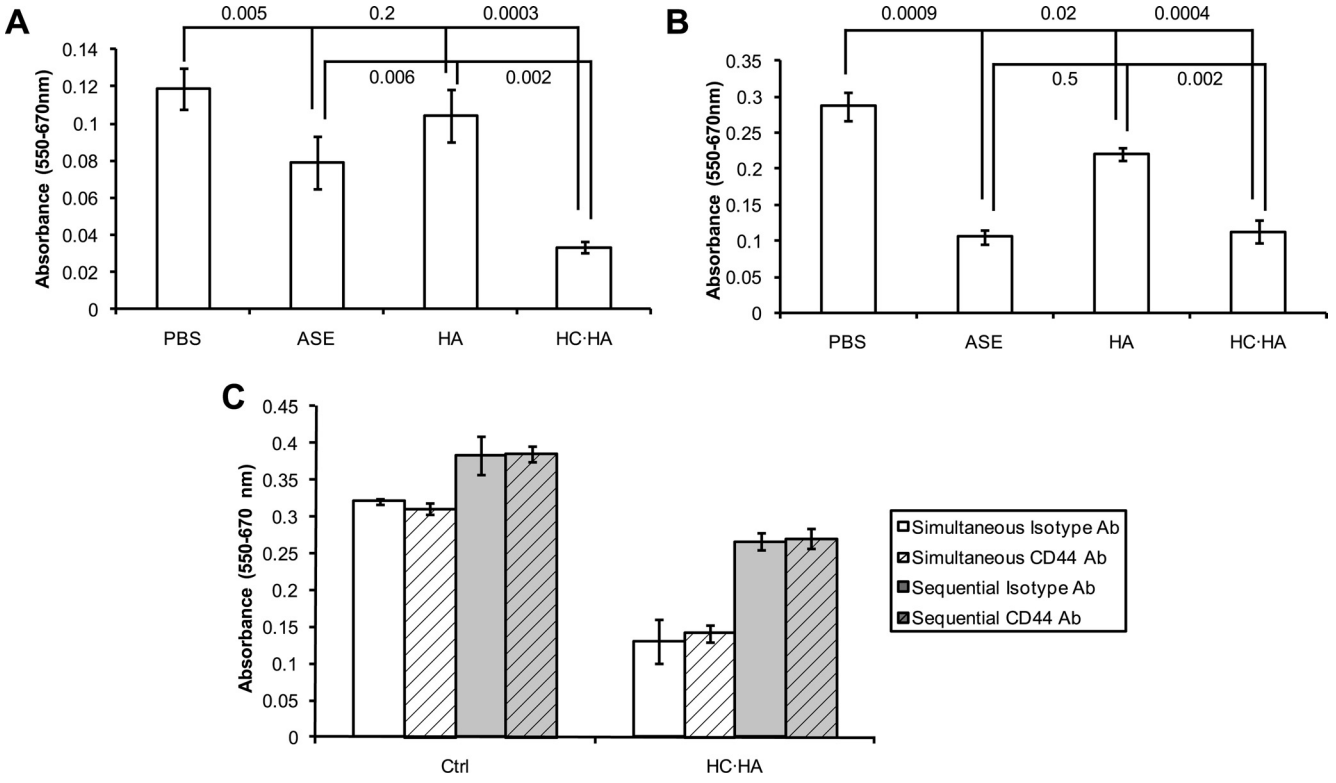

Figure 1. HC·HA suppresses HUVEC viability independently of CD44. HUVECs were treated with PBS, 200 μg/mL ASE, 5 μg/mL HA, or 5 μg/mL (**A**, **B**) or 25 μg/mL (**C**) HC·HA before the MTT assay. When added simultaneously to seeding (**A**), HC·HA and ASE, but not HA, significantly inhibited viability; HC·HA was more potent than ASE. When added 24 hours after seeding (**B**), HC·HA, ASE, and HA significantly inhibited cell viability; HC·HA and ASE were more potent than HA. When simultaneously added to seeding or added 24 hours after seeding (**C**), viability suppressed by HC·HA could not be counteracted by a CD44 neutralizing antibody (IM7) when compared with a rat IgG2b isotype control antibody. Data were reported as mean ± SD ($n = 3$) for statistical analysis. *P* values are shown.

control ($P = 0.005$ and $P = 0.0003$, respectively; Fig. 1A). In contrast, 5 μg/mL HA did not cause any significant inhibition ($P = 0.2$). Furthermore, HC·HA significantly inhibited HUVEC viability more than did ASE and HA ($P = 0.002$ and $P = 0.006$, respectively). Cells were also seeded at 2000 and 4000 cells/well for 24 hours before the addition of ASE, HA, or HC·HA. MTT assay revealed that all three treatments significantly suppressed HUVEC viability at the low seeding density (2000 cells/well) (Fig. 1B; $P = 0.009$, $P = 0.02$, and $P = 0.0004$, respectively). Suppression by ASE and HC·HA was significantly greater than by HA ($P = 0.0001$ and $P = 0.002$, respectively), whereas that by ASE and HC·HA was not significantly different ($P = 0.5$). At the high seeding density (4000 cells/well), both ASE and HC·HA significantly suppressed HUVEC viability ($P = 0.007$ and $P = 0.01$, respectively), whereas HA did not ($P = 0.1$). The difference between the low and the high seeding density in inhibiting HUVEC viability by 5 μg/mL HA was likely due to the fact that HA inhibition required a higher concentration and was less potent than that of HC·HA.

To test whether the inhibition of HUVEC viability by HC·HA was mediated by a well-known HA receptor, CD44, we added a CD44 blocking antibody before the MTT assay. Consistent with the above MTT data, HC·HA significantly suppressed cell viability when added simultaneously or sequentially with cell seeding ($P = 0.0008$ and $P = 0.006$, respectively; Fig. 1C), with the former more effective than the latter ($P = 0.008$). However, CD44 blocking antibody did not significantly alter the inhibitory activity of HC·HA when added simultaneously or sequentially ($P = 0.6$ and $P = 0.8$, respectively). Collectively, these results indicated that HC·HA suppressed HUVEC viability more so than ASE or HA and that this suppression was not mediated by CD44.

Determination of Angiogenic or Antiangiogenic Factors in HC·HA Complex

Many antiangiogenic factors are present in human AM. For example, PEDF, a potent antiangiogenic factor,[26] was predominantly found in the AM basement membrane.[27] Transcripts and proteins of tissue inhibitors of metalloproteinase and transcript of TSP-1 (i.e., potential antiangiogenic factors) are expressed by both human amniotic epithelial and mesenchymal cells.[28] To determine whether HC·HA antiangiogenic action might be contributed by PEDF or TSP-1, we performed Western blot analysis. Our results (Fig. 2A) showed that although PEDF was detected in the AM extract (lane 1) and in the pooled fractions after F1 (lane 2), it was not present in the pooled fractions after F2 (lane 3) or HC·HA (lane 4). As for TSP-1, it was not present in the AM extract (prepared in PBS) and HC·HA (data not shown). To further determine whether other factors might be present in the HC·HA complex, we used human angiogenesis arrays, which contained 56 individual human angiogenic and antiangiogenic factors, including PEDF, TSP-1, and TSP-2. The array data revealed there were at least 19 angiogenic factors, including PEDF, in the AM extract. In contrast, only insulin-like growth factor binding protein-1 (IGFBP-1) and platelet factor 4 (PF4 or CXCL4) were clearly, whereas IGFBP-2, IGFBP-3, and tissue inhibitor 1 of metalloproteinase (TIMP-1) were weakly detected in the HC·HA complex (Fig. 2B). Interestingly, the amount of IGFBP-1 in the HC·HA complex was even more than that in the AM extract (1.4 ± 0.07-fold), whereas the amount of PF4 in the HC·HA complex was about the same as that in the AM extract (1.1 ± 0.03-fold) (Fig. 2C). These data suggest that IGFBP-1 and PF4 might be truly bound tightly to the HC·HA complex.

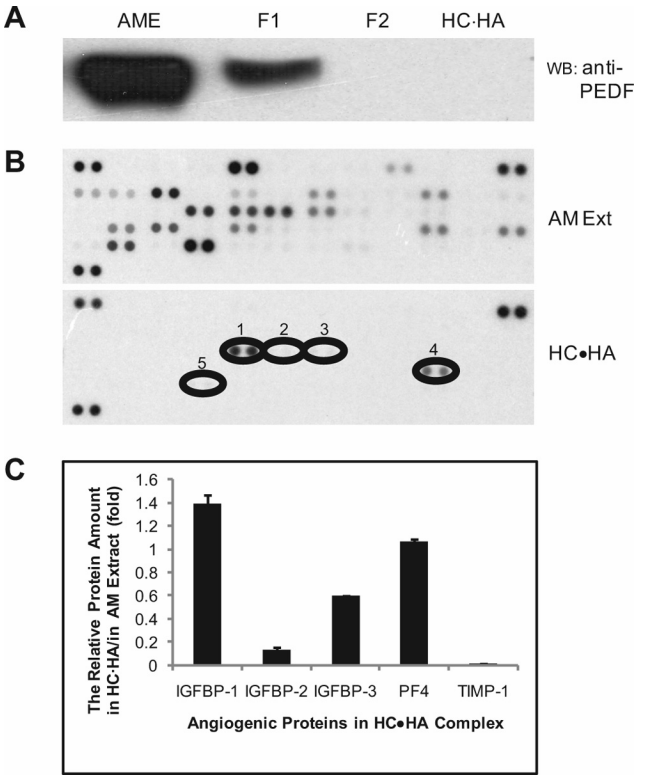

FIGURE 2. Detection of human angiogenic and antiangiogenic factors in the HC·HA complex by Western blot and protein arrays. (**A**) Western blot. 2 μg HA in AM extract, pooled fractions after F1 and F2, and HC·HA (each containing 2 μg HA) were loaded to each well and electrophoresed on 4% to 15% (wt/vol) gradient acrylamide gels under denaturing and reducing conditions. Proteins were transferred to the nitrocellulose membrane, and the membrane was incubated sequentially with PEDF antibodies and the respective secondary antibody. Detection was enhanced with reagent. (**B**) Protein arrays. 1.5 mL (25 μg/mL HA) AM extract or purified HC·HA complex was mixed with the detection antibodies, followed by incubation with the individual blocked human angiogenesis array membrane overnight at 4°C. After wash, each membrane was incubated with the secondary antibody, and signals were detected with chemiluminescent light exposed to x-ray films. Ovals labeled with numbers indicated candidate proteins detected in HC·HA. 1, 2, and 3: insulin-like growth factor binding protein-1, -2, and -3 (IGFBP-1,-2, and -3), respectively. 4: platelet factor 4 (PF4) or CXCL4. 5: TIMP-1. (**C**) Relative quantitation of candidate proteins in the HC·HA complex. The array data on developed x-ray film were quantitated by scanning the film on a transmission-mode scanner, and the array image file was analyzed by image analysis software (Image J). The relative protein amount in the HC·HA complex was compared with that in AM. The extract was set as 1.0.

HC·HA Dramatically Changed HUVEC Morphology, Reduced Cell Density, and Downregulated Filamentous Actin

We then examined whether the aforementioned suppression of cell viability by HC·HA might be accompanied by changes in cell morphology and density. HUVECs treated with 25 μg/mL HA maintained the same polyhedral shape and high cell density as the PBS control after 48 hours of culturing. In contrast, 25 μg/mL HC·HA rendered HUVECs small, rounded, and aggregated, with a notable decrease of cell density (Fig. 3A). F-actin detected by phalloidin staining showed organized actin filaments in the cytoplasm of the PBS control and HA-treated cultures (Fig. 3B; F-actin, green; nucleus, blue). In contrast, HC·HA–treated cells exhibited dramatically reduced F-actin with a decreased staining intensity. These results indicated that

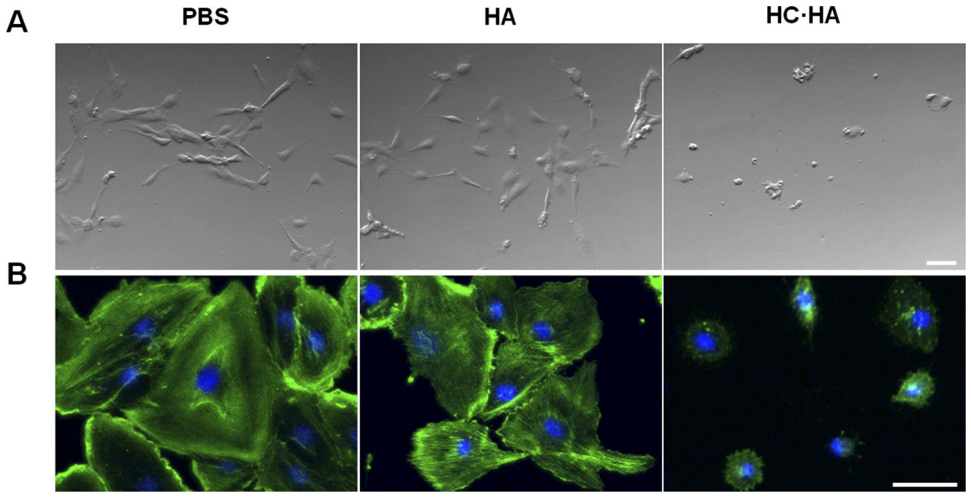

FIGURE 3. HC·HA alters HUVEC morphology, density, and F-actin. HUVECs were seeded at 1×10^4 cells per 8-well chamber slide with PBS, 25 μg/mL HA, or 25 μg/mL HC·HA. Phase-contrast micrographs taken 48 hours (**A**) after seeding showed adherent spindle cells in PBS- and HA-treated cultures but small, rounded, and aggregated cells with dramatically decreased cell numbers in HC·HA–treated cultures. F-actin staining (**B**) was extensive in PBS- and HMW HA-treated cells but significantly reduced in HC·HA–treated cells.

HC·HA suppressed HUVEC viability while slowing cell spreading by impairing the organization of the actin cytoskeleton.

HC·HA Dose Dependently Suppressed HUVEC Proliferation to a Greater Extent than HA without Promoting Cell Detachment or Death

Next we sought to determine whether suppression of the viability and alteration of the morphology and density by HC·HA were accompanied by the inhibition of cell proliferation. BrdU nuclear staining was similar for HUVECs seeded on plastic or treated with 25 μg/mL HA for 48 hours but was completely abolished if treated with 25 μg/mL HC·HA (Fig. 4A). BrdU ELISA further revealed that BrdU incorporation was not suppressed by HA at 1 to 50 μg/mL (all $P > 0.05$) but was significantly suppressed by HA only at 100 μg/mL ($P = 0.02$). In contrast, suppression of BrdU incorporation by HC·HA was significant at

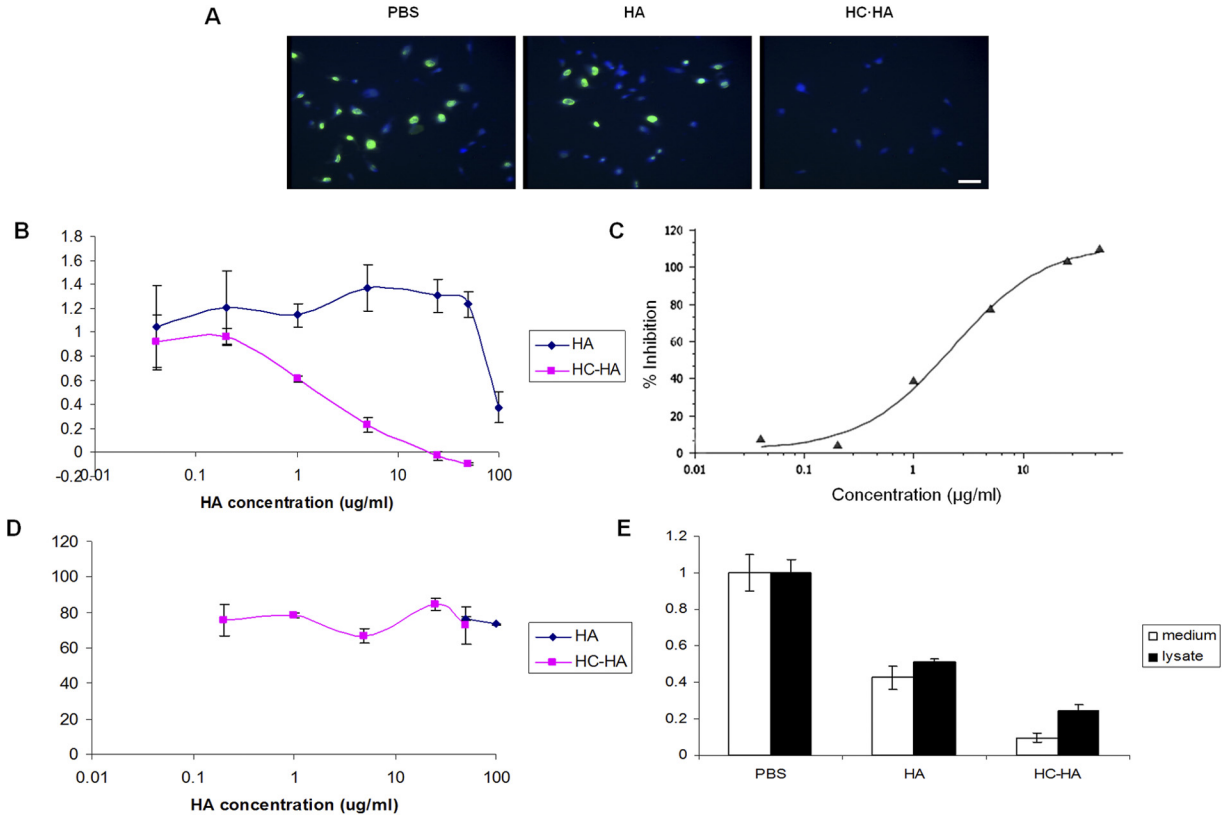

FIGURE 4. HC·HA inhibits HUVEC proliferation without causing cell detachment or death. HUVECs were seeded on uncoated chamber slides or FNC-coated 96-well dishes and treated with varying concentrations of HA or HC·HA in PBS for 48 hours. (**A**) Compared with PBS, BrdU nuclear labeling (*green*, BrdU; *blue*, Hoechst) on uncoated chamber slides was not affected by 25 μg/mL HA but was abolished by 25 μg/mL HC·HA. (**B**) BrdU incorporation on FNC-coated wells was significantly and dose dependently reduced by HC·HA from 1 to 50 μg/mL but not by HA. Values relative to PBS control set as as 1. (**C**) HC·HA inhibition of proliferation was dose dependent, with an IC_{50} value of 2.3 μg/mL. (**D**) Compared with the PBS control treated as 100%, HUVEC attachment was not affected by HA or HC·HA except at 50 μg/mL HC·HA. (**E**) Compared with the PBS control, HUVEC death was significantly reduced by HA in the lysate ($P = 0.02$), but not in the supernatant ($P = 0.07$), and was significantly reduced by HC·HA in both the supernatant ($P = 0.03$) and the lysate ($P = 0.005$).

0.04, 0.2, 1, 5, and 25 μg/mL ($P = 0.005$, $P = 0.02$, $P = 0.02$, $P = 0.02$, and $P = 0.0003$, respectively).

Because HC·HA changed cell morphology and reduced F-actin (Fig. 3)—and to ensure that the suppressive effect of HC·HA on proliferation was not influenced by cell attachment—we seeded HUVECs on FNC-coated plates to facilitate attachment while simultaneously adding 0.04 to 50 μg/mL HC·HA or 0.04 to 100 μg/mL HA. Similar to the uncoated plate, BrdU incorporation was not significantly affected by 0.04 to 50 μg/mL HA (all $P > 0.05$), but it was significantly affected by HA only at 100 μg/mL (Fig. 4B; $P = 0.005$). BrdU incorporation was also significantly inhibited by HC·HA from 1 to 50 μg/mL ($P = 0.004$, $P = 0.00008$, $P = 0.000007$, and $P = 0.0003$, respectively). Such suppression was dose dependent and revealed a linear semilogarithmic curve in which IC_{50} was found to be 2.3 μg/mL (R^2=0.99; Fig. 4C). Based on the HA molecular weight of ~3000 kDa,[12] we estimated that HC·HA was 100-fold more potent than HA. Importantly, cell attachment analyzed by the cell proliferation assay was not altered by either 25 to 50 μg/mL HA or 0.2 to 25 μg/mL HC·HA ($P > 0.5$ for all) but was affected by HC·HA only at 50 μg/mL ($P = 0.04$; Fig. 4D). These results collectively indicated that HC·HA was more potent than HA in inhibiting HUVEC proliferation in a dose-dependent manner and that such inhibition was not associated with the suppression of cell attachment.

Because HUVECs shrank to a small, round shape and cell density was notably reduced when treated with 25 μg/mL HC·HA (Fig. 3), we also tested whether the inhibition of cell proliferation was associated with cell death. Cell death detection (ELISA^{PLUS}) showed that compared with the PBS control, cell death measured in the culture supernatant was reduced by HC·HA more than by HA without a statistical difference on uncoated plates ($P = 0.2$ and $P = 0.07$, respectively); there was no difference between HA and HC·HA ($P = 0.3$). The cell death measured in the lysate caused by HA and HC·HA was also not significantly different from that of PBS control ($P = 0.1$ and $P = 0.1$, respectively). On FNC-coated plates, cell death measured in the supernatant (Fig. 4E, white bars) was significantly reduced by HC·HA ($P = 0.03$) but not by HA ($P = 0.07$) compared with the PBS control. Cell death measured in the lysate (Fig. 4E, black bars) was significantly reduced by both HA and HC·HA ($P = 0.02$ and $P = 0.005$, respectively). HC·HA significantly reduced cell death more than did HA ($P = 0.008$). These results collectively indicated that neither HA nor HC·HA promoted cell death. Instead, both of them, especially HC·HA, effectively protected HUVECs from undergoing apoptosis when cultured on FNC-coated plates.

HC·HA Inhibited Proliferation Stimulated by the Synergism between VEGF and Integrin Ligation

Proliferation depends on signals from growth factors and cues from the extracellular matrix. Thus, we sought to determine whether the antiangiogenic action of HC·HA could also counteract the synergism generated between VEGF and such substrates as Fn, Vn, and C.[29–32] Simultaneously with 25 μg/mL HC·HA, we seeded HUVECs in ECGM supplemented with 10 ng/mL VEGF onto plates coated with Fn, Vn, C, or FNC. BrdU ELISA showed that all substrates except Vn stimulated HUVEC proliferation compared with the uncoated control (Fig. 5; $P = 0.006$, $P = 0.006$, and $P = 0.01$ for Fn, C, and FNC, respectively, but $P = 0.3$ for Vn). However, on uncoated plastic and all four substrates, HC·HA significantly inhibited HUVEC proliferation (uncoated, $P = 0.0007$; Fn, $P = 0.001$; Vn, $P = 0.0008$; C, $P = 0.001$; FNC, $P = 0.004$). Thus, HC·HA still inhibited HUVEC proliferation even when proliferation was synergistically promoted by VEGF and such angiogenic substrates as Fn, Vn, and C.

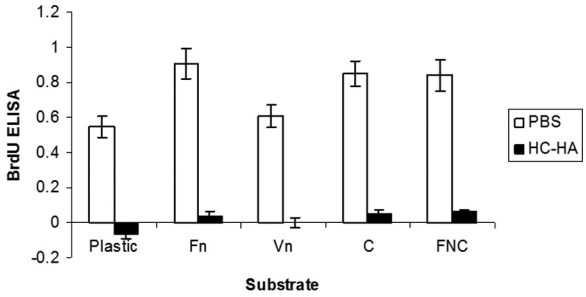

FIGURE 5. HC·HA inhibits HUVEC proliferation stimulated by both VEGF and angiogenic substrates. HUVECs were treated with or without 25 μg/mL HC·HA for 48 hours and were labeled with 10 μM BrdU for 6 hours before termination. BrdU ELISA showed that 25 μg/mL HC·HA markedly suppressed HUVEC proliferation stimulated by 10 μg/mL VEGF and cultured on uncoated plastic, Fn, Vn, C, and FNC ($n = 3$; $P = 0.0007$, $P = 0.001$, $P = 0.0008$, $P = 0.001$, and $P = 0.004$, respectively).

HC·HA Reduced HUVEC Migration toward VEGF as a Chemoattractant

Endothelial cell migration toward chemoattractants such as VEGF is a key step in angiogenesis. To determine whether HC·HA antiangiogenic action extended to HUVEC migration, we seeded HUVECs in the transwell assay using VEGF as a chemoattractant. HUVECs migrating from the upper chamber to the lower chamber were detected by crystal violet dye (Fig. 6A), and the number of migrated cells was counted (Fig. 6B). The results showed that HUVEC migration toward VEGF, when treated with HC·HA, was significantly less than that treated with HA or PBS (each $P = 0.05$). These findings indicated that HC·HA reduced HUVEC migration stimulated by VEGF.

HC·HA Suppressed HUVEC Tube Formation

To determine whether HC·HA antiangiogenic action extended to HUVEC differentiation into vascular structures in vitro, we seeded HUVECs onto extracellular matrix in ECGM with 10% FBS and 25 μg/mL HA or HC·HA. After 16 hours, HUVECs treated with PBS rapidly aligned and formed hollow, tubelike structures (Fig. 7A). In contrast, HUVECs treated with 25 μg/mL HC·HA showed a significant reduction of tube formation (Fig. 7B; $P = 0.0008$). As a comparison, HUVECs treated with 25 μg/mL HA did not reveal any significant difference from control ($P = 0.4$). Collectively, these results suggested that HC·HA also exerted its antiangiogenic actions by inhibiting HUVEC differentiation into tubelike structures during the angiogenic process.

HC·HA Suppressed Neovascularization in CAM

To determine whether the HC·HA complex also exerted antiangiogenic activity in vivo, we adopted CAM assay using fertilized White Leghorn chicken eggs incubated at 37.5°C with collagen onplants containing bFGF (16.7 μg/mL)/VEGF (5 μg/mL) with or without HA (1 μg/onplant) or HC·HA (1 μg/onplant) planted on day 8. After 4 days, the newly formed blood vessels into collagen onplants were recorded and quantitated. As shown in Figure 8A, bFGF/VEGF induced a robust growth of blood vessels growth into onplants. In contrast, both the HA and the HC·HA complexes apparently suppressed blood vessel formation into onplants; the large blood vessels formed adjacent to the onplant were suppressed by the HC·HA complex but not by HA. Compared with PBS, the suppression of neovascularization by both HA and the HC·HA complex was significant ($P = 0.02$ and $P = 0.01$, respectively). Although

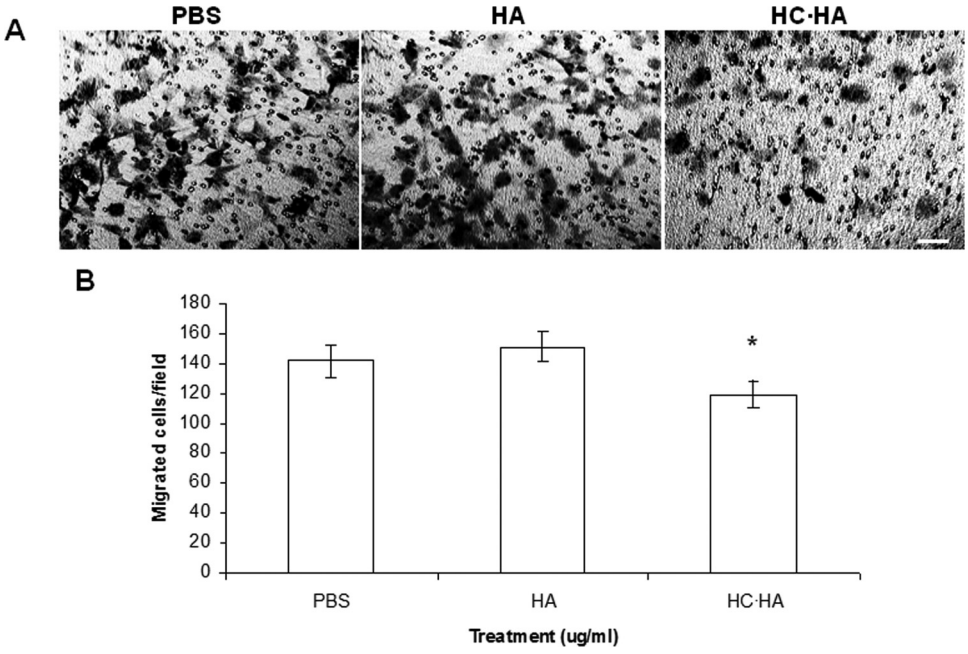

FIGURE 6. HC·HA reduces the chemotactic migration of HUVECs stimulated by VEGF. HUVECs were seeded in the upper well containing ECGM with PBS or 25 μg/mL HA or HC·HA, whereas 10 ng/mL VEGF was added to ECGM in the lower well as a chemoattractant. (**A**) Fewer migrated cells were found in HC·HA–treated cultures according to representative micrographs (**A**; scale bar, 50 μm) and cell numbers counted per field (**B**; minimum of five fields per group). $^*P < 0.05$ compared with the PBS control.

suppression by the HC·HA complex was more than that by HA, the difference was not significant ($P = 0.28$) (Fig. 8B).

DISCUSSION

Cumulative clinical experience attests that AM transplantation promotes epithelial wound healing while delivering anti-inflammatory, anti-scarring, and antiangiogenic actions to the ocular surface (see Refs. 6–10 for reviews). In the pursuit of the molecular mechanism whereby AM exerts the therapeutic actions mentioned, we recently purified the HC·HA complex from AM extract and demonstrated that this complex exerts an anti-scarring effect on cultured human corneal fibroblasts and an anti-inflammatory effect on cultured mouse macrophages.[12] The present study further adds that the HC·HA complex exerts a potent antiangiogenic effect on cultured HUVECs and CAM.

Angiogenesis involves the activation of vascular endothelium or endothelial progenitor cells through a series of cellular events including survival, migration, proliferation, and tube formation. Kobayashi et al.[33] noted that the conditioned medium of cultured amniotic epithelial and mesenchymal cells contains antiangiogenic activity, though the source of this activity remains obscure. The finding that ASE, which did not contain epithelial or basement membrane components, suppressed HUVEC viability (Fig. 1) was in agreement with previous findings by Jiang et al.[11] PEDF, a potent antiangiogenic

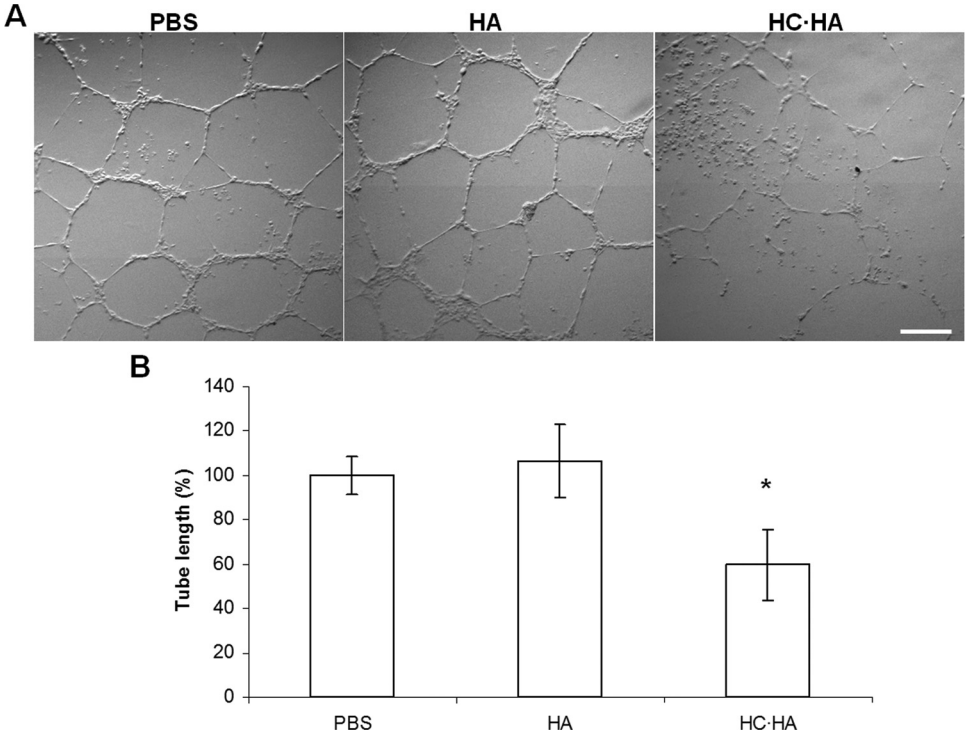

FIGURE 7. HC·HA inhibits HUVEC tube formation. HUVECs were seeded in ECGM supplemented with 10% FBS on extracellular matrix and were treated with PBS or 25 μg/mL HA or HC·HA for 16 hours. Fewer tube formations were found in HC·HA–treated cultures based on representative phase-contrast micrographs (**A**; scale bar, 200 μm) and (**B**) total length of tube formations per field in five random 100× fields (**B**, expressed as percentage of the PBS control treated as 100%). $^*P < 0.05$ compared with PBS.

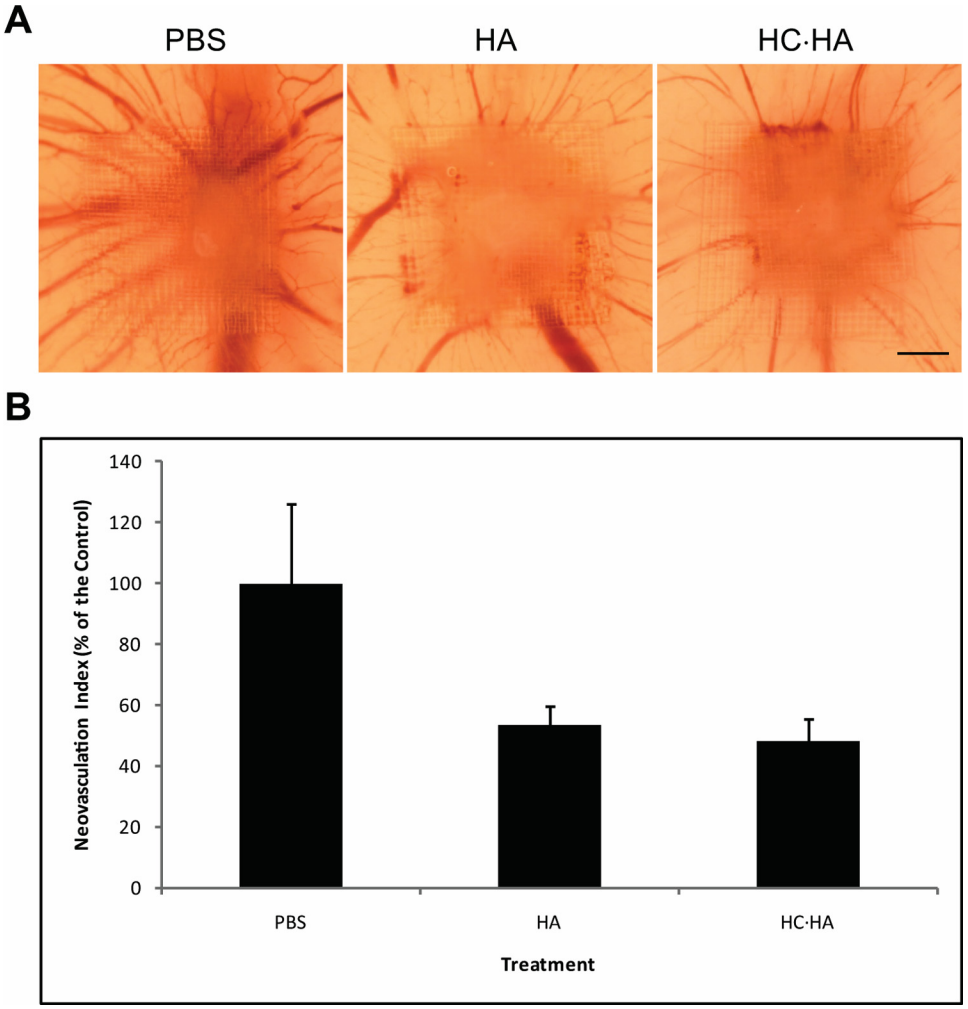

FIGURE 8. HC·HA suppresses neovascularization in CAM. Collagen onplants supplemented with bFGF (16.7 μg/mL) and VEGF (5 μg/mL) with the vehicle PBS control, high molecular weight HA (1 μg/onplant), or HC·HA (1 μg/onplant) were planted on CAM on day 8 of fertilized chick embryo (n = 7 each). Four days later, each CAM was fixed with 0.5 mL of 25% glutaraldehyde, photographed, and subjected to vessel quantitation. (**A**) One representative photograph from each group of control (PBS), HA, and HC·HA was shown. Scale bar, 1 mm. (**B**) Neovascularization was measured by counting the amount of blood vessels growing the each collagen onplants. Data were represented as the mean ± SD.

factor,[26] was predominantly found in the AM basement membrane.[27] Transcripts and proteins of tissue inhibitors of metalloproteinase and TSP-1—i.e., potential antiangiogenic factors—are expressed by both human amniotic epithelial and mesenchymal cells.[28] However, the roles of these three proteins in delivering antiangiogenic action in the AM cannot be ascertained because their protein levels are negligible in the medium after the incubation of human AM.[34] Our Western blot analysis showed that PEDF was present in the AM extract but not in the purified HC·HA complex (Fig, 2A), but TSP-1 was present in neither AM extract nor purified HC·HA (not shown). These results from Western blot analysis were further confirmed by the data of human angiogenesis arrays (Fig. 2B). Collectively, we conclude that the antiangiogenic action of the HC·HA complex, exerted by reducing HUVEC viability, proliferation, migration, and differentiation, is more potent than that of ASE and is not contributed by PEDF and TSP-1. Herein, our protein arrays showed that IGFBP-1, PF4, or both were selectively bound to the HC·HA complex (Figs. 8B, 8C). Previously, IGFBP-1[35,36] has been shown to suppress cell growth and PF4[37–39] has been shown to mediate antiangiogenic action. Thus, further studies are needed to determine whether the antiangiogenic actions of these two proteins are promoted by their binding to the HC·HA complex.

This HC·HA complex contains HA, which has been shown to promote cell quiescence and to exert anti-inflammatory and antiangiogenic effects.[21–24] Several studies have noted that HA is antiangiogenic through the inhibition of endothelial cell proliferation, migration, cell-cell adhesion, and tube formation.[40,41] In chicken embryo, the surrounding regions of HA-implanted wing buds are avascular.[42] HA also inhibits the formation and vascularization granulation tissue, the vascularization of implanted fibrin gels, and the angiogenic activity of human wound fluids in CAM assay (see Ref. 41 for review). Herein, our finding that HA at 100 μg/mL, but not at 50 μg/mL or less, could significantly inhibit HUVEC proliferation (Fig. 4) and CAM neovascularization was in agreement with the finding of an earlier study in which HA at concentrations greater than 100 μg/mL inhibited endothelial cell proliferation and disrupted confluent endothelial monolayers.[43] Our study showed that in addition to anti-scarring and anti-inflammatory effects,[12] HC·HA exerted a more potent antiangiogenic effect than HA. Specifically, HC·HA was 100-fold more potent than HA and dose dependently suppressed HUVEC proliferation with an IC_{50} of 2.3 μg/mL (Fig. 4).

Additionally, we found that HUVEC proliferation inhibited by the HC·HA complex was associated with a notable morphologic change characterized by the reduction of F-actin (Fig. 3). Reorganization of the F-actin cytoskeleton and cell-matrix adhesion play crucial roles in endothelial cell proliferation and migration in angiogenesis. Interestingly, this morphologic change linked to F-actin reorganization led to reduced cell density but did not promote cell detachment or death (Fig. 3). In fact, such HC·HA complex-treated cells exhibited reduced cell death by apoptosis on uncoated and FNC-coated plates, in some instances to a greater extent than HA (Fig. 4), suggesting that the HC·HA complex did not disassemble the entire actin-mediated cytoskeleton. Nonetheless, the HC·HA complex

downregulation of the actin cytoskeleton was sufficient to reduce HUVEC proliferation augmented by a synergistic action between VEGF and different substrates (Fig. 5) and HUVEC migration in response to VEGF (Fig. 6). Furthermore, we observed a decrease in tube formation (Fig. 7) that required the remodeling of actin filaments.[44] Because all these unique actions of HC·HA complex were not seen when HUVECs were treated with HA, because the HC·HA complex was 100-fold more potent than HA in suppressing HUVEC proliferation, and because the suppressive effect of the HC·HA complex in HUVEC viability could not be eliminated by a neutralizing antibody against CD44 (Fig. 1), we speculate that the HC·HA complex acts differently from HA in exerting its potent antiangiogenic action. This notion was further suggested in our preliminary data (not shown) showing that macrophages bound to immobilized HC·HA but not to immobilized HA, resulting in notable changes in proliferation and differentiation. Further studies in understanding how the HC·HA complex may bind to the cell membrane to cause the reorganization of actin filaments and subsequent signaling will help unravel the exact molecular action mechanism of this heretofore unknown antiangiogenic activity of the HC·HA complex. It should be noted that angiogenesis is a complex process and that our present study focuses only on the antiangiogenic action of the HC·HA complex on HUVECs in vitro and on the neovascularization on CAM in vivo. Further proof of such an action in vivo using other animal models is warranted. Such studies will not only shed light on how AM is developmentally avascular, they will also lead us to develop new therapeutics based on the HC·HA complex for treating such diseases as age-related macular degeneration, diabetic retinopathy, retinopathy of prematurity, rubeosis iridis in secondary glaucoma, and corneal neovascularization in which pathogenic angiogenesis prevails and causes blindness in humans.

References

1. Kruse FE, Joussen AM, Rohrschneider K, et al. Cryopreserved human amniotic membrane for ocular surface reconstruction. *Graefe's Arch Clin Exp Ophthalmol.* 2000;238:68–75.
2. Kim JC, Tseng SCG. The effects on inhibition of corneal neovascularization after human amniotic membrane transplantation in severely damaged rabbit corneas. *Korean J Ophthalmol.* 1995;9:32–46.
3. Tseng SCG, Prabhasawat P, Barton K, Gray T, Meller D. Amniotic membrane transplantation with or without limbal allografts for corneal surface reconstruction in patients with limbal stem cell deficiency. *Arch Ophthalmol.* 1998;116:431–441.
4. Tsubota K, Satake Y, Kaido M, et al. Treatment of severe ocular surface disorders with corneal epithelial stem-cell transplantation. *N Engl J Med.* 1999;340:1697–1703.
5. Tsai RJF, Li L-M, Chen J-K. Reconstruction of damaged corneas by transplantation of autologous limbal epithelial cells. *N Engl J Med*. 2000;343:86–93.
6. Sippel KC, Ma JJK, Foster CS. Amniotic membrane surgery. *Curr Opin Ophthalmol.* 2001;12:269–281.
7. Tseng SCG. Amniotic membrane transplantation for ocular surface reconstruction. *Biosci Rep.* 2002;21:481–489.
8. Dua HS, Gomes JA, King AJ, Maharajan VS. The amniotic membrane in ophthalmology. *Surv Ophthalmol.* 2004;49:51–77.
9. Bouchard CS, John T. Amniotic membrane transplantation in the management of severe ocular surface disease: indications and outcomes. *Ocul Surface.* 2004;2:201–211.
10. Tseng SCG, Espana EM, Kawakita T, et al. How does amniotic membrane work? *Ocul Surface.* 2004;2:177–187.
11. Jiang A, Li C, Gao Y, et al. In vivo and in vitro inhibitory effect of amniotic extraction on neovascularization. *Cornea.* 2006;25:S36–S40.
12. He H, Li W, Tseng DY, et al. Biochemical characterization and function of complexes formed by hyaluronan and the heavy chains of inter-α-inhibitor (HC·HA) purified from extracts of human amniotic membrane. *J Biol Chem.* 2009;284:20136–20146.
13. Fulop C, Szanto S, Mukhopadhyay D, et al. Impaired cumulus mucification and female sterility in tumor necrosis factor-induced protein-6 deficient mice. *Development.* 2003;130:2253–2261.
14. Jessen TE, Odum L. Role of tumour necrosis factor stimulated gene 6 (TSG-6) in the coupling of inter-alpha-trypsin inhibitor to hyaluronan in human follicular fluid. *Reproduction.* 2003;125:27–31.
15. Rugg MS, Willis AC, Mukhopadhyay D, et al. Characterization of complexes formed between TSG-6 and inter-alpha-inhibitor that act as intermediates in the covalent transfer of heavy chains onto hyaluronan. *J Biol Chem.* 2005;280:25674–25686.
16. Li W, He H, Kawakita T, Espana EM, Tseng SCG. Amniotic membrane induces apoptosis of interferon-gamma activated macrophages in vitro. *Exp Eye Res.* 2006;82:282–292.
17. He H, Li W, Chen SY, et al. Suppression of activation and induction of apoptosis in RAW264.7 cells by amniotic membrane extract. *Invest Ophthalmol Vis Sci.* 2008;49:4468–4475.
18. Kawakita T, Espana EM, He H, et al. Keratocan expression of murine keratocytes is maintained on amniotic membrane by downregulating TGF-beta signaling. *J Biol Chem.* 2005;280:27085–27092.
19. Kawakita T, Espana EM, He H, et al. Preservation and expansion of the primate keratocyte phenotype by downregulating TGF-beta signaling in a low-calcium, serum-free medium. *Invest Ophthalmol Vis Sci.* 2006;47:1918–1927.
20. Ochsner SA, Day AJ, Rugg MS, Breyer RM, Gomer RH, Richards JS. Disrupted function of tumor necrosis factor-alpha-stimulated gene 6 blocks cumulus cell-oocyte complex expansion. *Endocrinology.* 2003;144:4376–4384.
21. McKee CM, Penno MB, Cowman M, et al. Hyaluronan (HA) fragments induce chemokine gene expression in alveolar macrophages: the role of HA size and CD44. *J Clin Invest.* 1996;98:2403–2413.
22. Rooney P, Wang M, Kumar P, Kumar S. Angiogenic oligosaccharides of hyaluronan enhance the production of collagens by endothelial cells. *J Cell Sci.* 1993;105(pt 1):213–218.
23. Morrison H, Sherman LS, Legg J, et al. The NF2 tumor suppressor gene product, merlin, mediates contact inhibition of growth through interactions with CD44. *Genes Dev.* 2001;15:968–980.
24. Slevin M, Krupinski J, Gaffney J, et al. Hyaluronan-mediated angiogenesis in vascular disease: uncovering RHAMM and CD44 receptor signaling pathways. *Matrix Biol.* 2007;26:58–68.
25. Han YS, Lee JE, Jung JW, Lee JS. Inhibitory effects of bevacizumab on angiogenesis and corneal neovascularization. *Graefes Arch Clin Exp Ophthalmol.* 2009;247:541–548.
26. Stellmach V, Crawford SE, Zhou W, Bouck N. Prevention of ischemia-induced retinopathy by the natural ocular antiangiogenic agent pigment epithelium-derived factor. *Proc Natl Acad Sci U S A.* 2001;98:2593–2597.
27. Shao C, Sima J, Zhang SX, et al. Suppression of corneal neovascularization by PEDF release from human amniotic membranes. *Invest Ophthalmol Vis Sci.* 2004;45:1758–1762.
28. Hao Y, Ma DH-K, Hwang DG, Kim WS, Zhang F. Identification of antiangiogenic and antiinflammatory proteins in human amniotic membrane. *Cornea.* 2000;19:348–352.
29. Kim S, Bell K, Mousa SA, Varner JA. Regulation of angiogenesis in vivo by ligation of integrin alpha5beta1 with the central cell-binding domain of fibronectin. *Am J Pathol.* 2000;156:1345–1362.
30. Schwartz MA, Assoian RK. Integrins and cell proliferation: regulation of cyclin-dependent kinases via cytoplasmic signaling pathways. *J Cell Sci.* 2001;114:2553–2560.
31. Hood JD, Frausto R, Kiosses WB, Schwartz MA, Cheresh DA. Differential αv integrin-mediated Ras-ERK signaling during two pathways of angiogenesis. *J Cell Biol.* 2003;162:933–943.
32. Wijelath ES, Rahman S, Namekata M, et al. Heparin-II domain of fibronectin is a vascular endothelial growth factor-binding domain: enhancement of VEGF biological activity by a singular growth factor/matrix protein synergism. *Circ Res.* 2006;99:853–860.
33. Kobayashi N, Kabuyama Y, Sasaki S, Kato K, Homma Y. Suppression of corneal neovascularization by culture supernatant of human amniotic cells. *Cornea.* 2002;21:62–67.

34. Ma DH, Yao JY, Yeh LK, et al. In vitro antiangiogenic activity in ex vivo expanded human limbocorneal epithelial cells cultivated on human amniotic membrane. *Invest Ophthalmol Vis Sci.* 2004;45: 2586–2595.
35. Ben LN, Seurin D, Le BY, et al. Insulin-like growth factor binding protein (IGFBP-1) involvement in intrauterine growth retardation: study on IGFBP-1 overexpressing transgenic mice. *Endocrinology.* 2006;147:4730–4737.
36. Watson CS, Bialek P, Anzo M, Khosravi J, Yee SP, Han VK. Elevated circulating insulin-like growth factor binding protein-1 is sufficient to cause fetal growth restriction. *Endocrinology.* 2006;147:1175–1186.
37. Hagedorn M, Zilberberg L, Lozano RM, et al. A short peptide domain of platelet factor 4 blocks angiogenic key events induced by FGF-2. *FASEB J.* 2001;15:550–552.
38. Jouan V, Canron X, Alemany M, et al. Inhibition of in vitro angiogenesis by platelet factor-4-derived peptides and mechanism of action. *Blood.* 1999;94:984–993.
39. Maione TE, Gray GS, Petro J, et al. Inhibition of angiogenesis by recombinant human platelet factor-4 and related peptides. *Science.* 1990;247:77–79.
40. Rooney P, Kumar S, Ponting J, Wang M. The role of hyaluronan in tumour neovascularization (review). *Int J Cancer.* 1995;60:632–636.
41. West DC, Fan PD. Hyaluronan oligosaccharides promote wound repair. In: Kohn EC, Fan PD, eds. *The New Angiotherapy*. Totowa, NJ: Humana Press; 2002:177–186.
42. Feinberg RN, Beebe DC. Hyaluronate in vasculogenesis. *Science.* 1983;220:1177–1179.
43. West DC, Kumar S. The effect of hyaluronate and its oligosaccharides on endothelial cell proliferation and monolayer integrity. *Exp Cell Res.* 1989;183:179.
44. Qian Y, Luo J, Leonard SS, et al. Hydrogen peroxide formation and actin filament reorganization by Cdc42 are essential for ethanol-induced in vitro angiogenesis. *J Biol Chem.* 2003;278:16189–16197.